Brown, *ibid.*, **93**, 5715 (1971); D. F. Eaton and T. G. Traylor, *ibid.*, **96**, 1226 (1974); and prior references cited in those papers.
(4) L. Radom, J. A. Pople, and P. v. R. Schleyer, *J. Am. Chem. Soc.*, **94**, 5935 (1972).
(5) G. A. Olah and R. J. Spear, *J. Am. Chem. Soc.*, **97**, 1539 (1975); G. A. Olah, C. L. Jeuell, D. P. Kelly, and R. D. Porter, *ibid.*, **94**, 146 (1972).
(6) J. J. Solomon and F. H. Field, *J. Am. Chem. Soc.*, **98**, 1567 (1976).
(7) G. A. Olah, A. M. White, J. R. DeMember, A. Commeyras, and C. Y. Lui, *J. Am. Chem. Soc.*, **92**, 4627 (1970); G. A. Olah, G. D. Mateescu, and J. L. Riemenschneider, *ibid.*, **94**, 2529 (1972).
(8) H. C. Brown, *Acc. Chem. Res.*, **6**, 377 (1973).
(9) For other experimental and theoretical work on the vinyl cation see J. Weber and A. D. McLean, *J. Am. Chem. Soc.*, **98**, 875 (1976); P. C. Hariharan, W. A. Lathan, and J. A. Pople, *Chem. Phys. Lett.*, **14**, 385 (1972); A. C. Hopkinson, K. Yates, and I. G. Csizmadia, *J. Chem. Phys.*, **55**, 3835 (1971); Z. Rappoport, I. Schnabel, and P. Greenzaid, *J. Am. Chem. Soc.*, **98**, 7726 (1976), and references cited therein; P. J. Stang, *Prog. Phys. Org. Chem.*, **10**, 205 (1973).
(10) This limitation has long been known. For a recent review and discussion applied to Walsh's rules, see R. J. Buenken and S. D. Peyerimhoff, *Chem. Rev.*, **74**, 127 (1974). E. R. Davidson [*J. Chem. Phys.*, **57**, 1999 (1972)] has defined an alternative set of canonical orbitals within the Roothaan–Hartree–Fock formalism and has shown [L. Z. Stenkamp and E. R. Davidson, *Theor. Chim. Acta*, **30**, 283 (1973)] how such SCF orbital energies can be applied to molecular changes of the Walsh type.
(11) R. Hoffmann, *J. Chem. Phys.*, **39**, 1197 (1963); R. Hoffmann, R. Piccioni, and R. Fahey, Program No. 48, QCPE, Indiana University, Bloomington, Ind.
(12) W. J. Hehre, R. F. Stewart, and J. A. Pople, *J. Chem. Phys.*, **51**, 2657 (1969).
(13) W. J. Hehre, W. A. Lathan, R. Ditchfield, M. D. Newton, and J. A. Pople, Program No. 236, QCPE, Indiana University, Bloomington, Ind.
(14) A. Streitwieser, Jr., P. H. Owens, R. A. Wolf, and J. E. Williams, *J. Am. Chem. Soc.*, **96**, 5448 (1974); P. H. Owens and A. Streitwieser, Jr., *Tetrahedron*, **27**, 4471 (1971).
(15) H. A. Bent, *Chem. Rev.*, **61**, 275 (1961).
(16) A. Streitwieser, Jr., J. M. McKelvey, and A. G. Toczko, in preparation; for a specific example, see A. Streitwieser, Jr., J. E. Williams, Jr., S. Alexandratos, and J. M. McKelvey, *J. Am. Chem. Soc.*, **98**, 4778 (1976).
(17) J. E. Williams and A. Streitwieser, Jr., *Chem. Phys. Lett.*, **25**, 507 (1974); P. Politzer and R. R. Harris, *J. Am. Chem. Soc.*, **92**, 6451 (1970); R. S. Mulliken, *J. Chem. Phys.*, **36**, 3428 (1962).
(18) O. Bastiansen and M. Traetteberg, *Tetrahedron*, **17**, 147 (1962).
(19) L. Radom, W. A. Lathan, W. J. Hehre, and J. A. Pople, *J. Am. Chem. Soc.*, **93**, 5339 (1971).
(20) L. Radom, J. A. Pople, V. Buss, and P. v. R. Schleyer, *J. Am. Chem. Soc.*, **94**, 311 (1972); P. C. Hariharan, L. Radom, J. A. Pople, and P. v. R. Schleyer, *ibid.*, **96**, 599 (1974).
(21) J. A. Pople and M. S. Gordon, *J. Am. Chem. Soc.*, **89**, 4253 (1967).
(22) L. Radom, *Aust. J. Chem.*, **27**, 231 (1974).
(23) W. J. Hehre, R. T. McIver, J. A. Pople, and P. v. R. Schleyer, *J. Am. Chem. Soc.*, **96**, 7162 (1974).
(24) J. L. Devlin III, J. F. Wolf, R. W. Taft, and W. J. Hehre, *J. Am. Chem. Soc.*, **98**, 1990 (1976).
(25) J. M. McKelvey, S. Alexandratos, A. Streitwieser, Jr., J. L. M. Abboud, and W. J. Hehre, *J. Am. Chem. Soc.*, **98**, 244 (1976).

A Theoretical Relation for the Position of the Energy Barrier between Initial and Final States of Chemical Reactions

Arnold R. Miller[1]

Contribution from the Department of Chemistry, State University of New York at Stony Brook, Stony Brook, New York 11794. *Received December 29, 1975; revised and expanded July 25, 1977.*

Abstract: A function ψ is derived that approximates the potential-energy barrier position x^*_0 of elementary reactions in terms of the barrier height U^* and reaction potential energy U_f. The functional expression is $x^*_0 = 1/[2 - (U_f/U^*)]$, where x^*_0 is the value of the defined reaction coordinate x, $0 \leq x \leq 1$, that corresponds to the activated state; endpoints $x = 0$ and $x = 1$ correspond to the initial and final states, respectively. For three-body atom transfer reactions, x^*_0 is equal to the activated-complex bond order of the bond being formed. The central idea of the derivation is a proposition that the most realistic global interpolating function of a family, all of whose members equally well interpolate the potential coordinate function of the vector equation describing the minimum-energy reaction path, is the unique member having the least arc length for its potential curve or graph. This criterion may be considered an abstract, generalized basis for the well-known Hammond postulate. Relation ψ is tested principally by (a) graphical comparison with analogous functions generated numerically from the bond-energy/bond-order (BEBO) and London–Eyring–Polanyi–Sato (LEPS) potential functions, and (b) comparison of the saddle-point coordinates computed by the function with those computed by other methods, including ab initio methods. Agreement is good, and, as a generalization, the relation's predicted barrier position is very similar to that of the BEBO function.

Introduction

The position of the energy barrier over configuration space is one of the dynamically most important properties of a potential-energy surface.[2] Interest in the barrier position (i.e., the position of the barrier maximum) arises principally because of its profound effect on reaction rate. For example, the barrier position determines the *kind* of energy which will promote the reaction. Elementary three-body reactions having early barriers, or barriers in the entrance channel of the surface, are much more effectively promoted by reactant translational energy than vibrational energy, and, in striking cases, reactant vibrational energy even in excess of twice the barrier height gives no reactive trajectories whatever.[3] This effect of energy selectivity by the barrier position is of importance not only to the rates of elementary reactions but to the rates of (disequilibrium) reaction networks in which the reactant energy distribution for one elementary step is provided by the product energy distribution of the preceding step. That is, the rate of the network will depend in part on the relative barrier positions of the elementary steps. As another example, the rate acceleration of solvation depends strongly on the barrier position since the latter determines the structure and electrostatic charge of the activated state. For instance, it has been predicted for an ionogenic reaction (the Menschutkin reaction) that the rate enhancement accompanying a given change in solvent (all other variables held constant) will vary from a factor of 10 to a factor of 10^{10} depending on the barrier position.[4]

There is presently no unambiguous experimental method of determining the barrier position. Two experimental reaction parameters commonly related to the barrier position are the Brønsted slope[5] and the kinetic isotope effect.[6] However, the validity of these methods is generally uncertain because of the uncertainty of the multiple assumptions upon which they rest. The method nearest to being a bona fide experimental method involves the construction of an adjustable, semiempirical potential-energy surface that properly reproduces a given reaction's experimentally observed dynamics, for example, the

0002-7863/78/1500-1984$01.00/0

activation energy or product vibrational energy distribution. The barrier position of the resulting surface is then taken as an approximation to the true barrier position of the reaction. However, despite the method's laboriousness, it is not definitive. Sometimes no surface of a given kind can be found which satisfies the dynamical criteria.[7] In other cases, several acceptable surfaces meet the criteria,[8] and hence several widely divergent barrier positions are inferred.

The major theoretical work on the barrier position may be briefly narrated. Hammond[9] has stated a qualitative assumption, known widely as the Hammond postulate, regarding the general shape or geometric form of the potential curve of elementary reactions. The postulate, which is limited to reactions having small relative barriers in one direction, may be paraphrased as follows: if the activated complex is near in potential energy to an adjacent metastable state, then it is also near in structure to the same state. This assumption has played an important role in mechanistic organic chemistry,[10] particularly in the estimation of the structure of the activated complex from the structure of a metastable intermediate such as a carbonium ion. Polanyi[11] has treated the barrier-position problem in terms of a valence bond model in which the two bonds of a linear three-body complex are of equal energy. This treatment predicts in a general manner that the more endothermic a reaction, the later the barrier. Marcus,[12] in a generalization of his theory of electron transfer reactions to include atom transfers, has derived two expressions for a reaction's instantaneous Brønsted slope which are in terms of the intrinsic barrier (see below) and reaction energy. Since other parts of the treatment equate the Brønsted slope and one measure of activated-complex structure, the relations may be interpreted as giving a theoretical barrier position. Mok and Polanyi[13] have formulated an essentially qualitative, and in a sense empirical, generalization regarding the relationship between barrier position and barrier height in homologous series of reactions; the observation is based on the behavior of semiempirical bond-energy/bond-order (BEBO) and London–Eyring–Polanyi–Sato (LEPS) potential curves. The principal correlation is that the barrier occurs early for exothermic reactions and shifts to successively later positions as the barrier height increases within a series.

The purpose of this paper is to propose a general expression for the approximate elementary barrier position as a function of both the barrier height and reaction potential energy. The function is derived as the general optimization (arc length minimization) solution of a procedure for globally interpolating a reaction's potential coordinate function with a special class of functions. The derived relation, tested against other theoretical methods, including ab initio methods, compares favorably with the best of the methods for computing the barrier position.

Barrier Position Relation

The potential-energy hypersurface of an elementary reaction is a set of points in $(n + 1)$-dimensional configuration-energy space; each point represents the energy associated with one of all possible nuclear configurations of the system. The general point on the surface is $(r_1, r_2, \ldots, r_n, U)$, where the coordinates r_i, $i = 1, 2, \ldots, n$, represent the n internuclear distances sufficient to describe any configuration, and U is the corresponding potential energy. (Henceforth, a subscript i is reserved as an integer index understood to range over all appropriate values.) For a reaction involving m nuclei, the dimension n of configuration space is[14]

$$n = \begin{cases} 1 & \text{if } m = 2 \\ 3m - 6 & \text{if } m \geq 3 \end{cases} \tag{1}$$

The *minimum-energy reaction path* is the most probable course of the reacting system across the surface. It is the path crossing the surface from the initial state that allows the least energy for each successive point on the path. The general vector equation of the minimum-energy reaction path is

$$\mathbf{R}(x) = [r_1(x), r_2(x), \ldots, r_n(x), U(x)] \tag{2}$$

where $r_i(x)$ are the n internuclear distance coordinate functions; $U(x)$ is the potential coordinate function; and x, a scalar, is the parameter of the equation and has a range $0 \leq x \leq 1$. In this treatment, parameter x associated with the minimum-energy reaction path is defined and taken as the *reaction coordinate*, that is, a scalar measure of the extent of the elementary chemical event. A value of $x = 0$ represents the initial state of the system; $x = 1$ represents the final state. Scalar x has a specific, chemical interpretation in this method, although eq 2, as a vector equation, is parameterization independent. Since the essential meaning of chemical process, vis-à-vis physical process, is the making and breaking of chemical bonds, x is defined in terms of the bond order b of an index bond, or reference bond, that undergoes complete change during the reaction. Hence, $x = b$ if the index bond is being formed in the reaction, and $x = (1 - b)$ if the index bond is being broken in the reaction. Bond order is "chemist's bond order", which has been discussed elsewhere.[15]

For many reactions, the distance coordinate functions r_i are probably known. This is true for many three-body transfer reactions, a large and important class of elementary reactions having the general form

$$\mathrm{AB} + \mathrm{C} \rightarrow \mathrm{A} \cdots \mathrm{B} \cdots \mathrm{C} \rightarrow \mathrm{A} + \mathrm{BC} \tag{3}$$

where A, B, and C represent either atoms or groups. The specific reactions considered in this paper will be from this class. The following subscript convention is observed for variables associated with reaction 3: a subscript $i = 1$ refers to bond AB, $i = 2$ refers to bond BC, and $i = 3$ refers to the hypothetical isolated bond AC. Since $m = 3$, the vector equation of the minimum-energy reaction path of reaction 3 is

$$\mathbf{R}(x) = [r_1(x), r_2(x), r_3(x), U(x)] \tag{4}$$

The reaction coordinate x is equated to the bond order of the bond being formed, bond BC. For complexes on the minimum-energy reaction path, two special circumstances frequently obtain: (1) the total bond order around atom B is approximately constant and equal to unity, i.e., $b_1 + b_2 = 1$ (especially for B = hydrogen[15,16] in the gas phase but probably for other cases as well[17]), and (2) A, B, and C are collinear.[18] With these assumptions, the functions r_i in eq 4 are derived from Pauling's relation (a relation between bond order and bond length)[19] and the collinearity condition that $r_3 = r_1 + r_2$ to give

$$r_1(x) = \hat{r}_1 - \alpha \ln (1 - x) \tag{5}$$

$$r_2(x) = \hat{r}_2 - \alpha \ln x \tag{6}$$

$$r_3(x) = \hat{r}_1 + \hat{r}_2 - \alpha \ln (x - x^2) \tag{7}$$

where constants $\hat{r}_i$ are the equilibrium bond lengths in Å when $b_i = 1$, and parameter α, from Pauling's relation, is assigned the rounded value $\alpha = 0.26$. With the distance coordinate functions determined, the projection of path $\mathbf{R}$ onto configuration space,

$$\mathbf{R}_0(x) = [r_1(x), r_2(x), \ldots, r_n(x), 0] \tag{8}$$

the most probable path through configuration space, is known; the problem is to determine where along this path the barrier lies.

The *barrier position* for general reactions is defined as the value of reaction coordinate x, symbolized x^*, corresponding to the maximum of potential coordinate function U in eq 2.

That is, x^* is the maximum-point solution of

$$U'(x) = 0 \tag{9}$$

where U' is the first derivative of function U with respect to x. If functions r_i in eq 2 are known, the barrier position may additionally be described in terms of the saddle point coordinates $\mathbf{R}_0(x^*)$. An a priori, rigorous expression for eq 9 is not known for any reaction. Even if a general a priori expression were known, it probably would not be solvable for x^* to give a closed-form solution for the barrier position. The BEBO function[15] (see below) may be viewed in this context as a relatively simple approximation to $U(x)$. However, even the first derivative of the BEBO function cannot be explicitly solved for x^*. What is desired is to approximate $U(x)$ in a general manner with a function sufficiently convenient that an expression for the barrier position x^* can be derived.

The derivation of the barrier position relation is based on the global interpolation of function U with a special class of functions; the relation is derived as the general solution for the maximum point of such an interpolating function. The interpolating functions are two-piece, smooth (continuous first derivative), continuous functions of the class

$$f(x,x^*) = \begin{cases} g_1(x,x^*), & 0 \leqslant x \leqslant x^* \\ g_2(x,x^*), & x^* \leqslant x \leqslant 1 \end{cases} \tag{10}$$

that is, of the class of double-knot spline functions. Function $f(x,x^*)$ may be viewed as a function of two variables or, preferably, as a family of functions having x^* both as the single parameter of the family and as the junction point of each member. Aside from being required to satisfy the continuity and smoothness conditions on f, the only restriction on functions g_1 and g_2 is that they both belong to the same k-parameter family of functions. [*Definition:* two mathematical expressions in x belong to the same k-parameter family of functions if they each contain k functional parameters or coefficients (*i.e.*, they have k degrees of freedom), and they differ only by the values of the k parameters. For example, all second-degree polynomials belong to the same three-parameter family, and functions h_1 and h_2, where $h_1(x) = a_1 \sin(a_2x) + a_3 \exp(a_4x)$, $h_2(x) = b_1 \sin(b_2x) + b_3 \exp(b_4x)$, and the a's and b's are the functional parameters, belong to the same four-parameter family.] Therefore, in order to determine g_1 and g_2 uniquely (and hence function f), for each there must be k interpolation conditions that both $g_i(x)$ and $U(x)$, or the respective derivatives, satisfy simultaneously.

The only general conditions on function U, the interpolation conditions function f must satisfy, are displayed in eq 11-16

$$U(0) = f(0,x^*) = 0 \tag{11}$$

$$U'(0) = f'(0,x^*) = 0 \tag{12}$$

$$U(x^*) = f(x^*,x^*) = U^* \tag{13}$$

$$U'(x^*) = f'(x^*,x^*) = 0 \tag{14}$$

$$U(1) = f(1,x^*) = U_f \tag{15}$$

$$U'(1) = f'(1,x^*) = 0 \tag{16}$$

where the relative potential energy of the initial state ($x = 0$) is taken as zero; U' and f' are the first derivatives with respect to x; U^* is the maximum of U, the barrier height; and U_f is the relative potential energy of the final state. It is noteworthy that the BEBO function, due to the form of its bonding potential functions, does not have stationary endpoints as required by eq 12 and 16. However, if the standard Morse function were written in terms of x via Pauling's relation and taken as the bonding functions, then the function would have stationary endpoints.[20] It will be assumed that function U is realistically described by all six conditions 11-16. However, as will be shown below, this assumption is not essential to the conclusion of the paper.

Two examples of interpolating functions satisfying the above conditions are f_1 and f_2 (eq 17 and 18).

$$f_1(x,x^*) = \begin{cases} U^*(-2x^3 + 3x^2x^*)/x^{*3} & 0 \leqslant x \leqslant x^* \\ (U^* - U_f)[-2x^3 + 3(x^* + 1)x^2 \\ \quad - 3x^*(2x - 1) - 1]/(x^* - 1)^3 + U_f & x^* \leqslant x \leqslant 1 \end{cases} \tag{17}$$

$$f_2(x,x^*) = \begin{cases} (\cos[\pi\,(x - x^*)/x^*] + 1)U^*/2 & 0 \leqslant x \leqslant x^* \\ (\cos[\pi(x - x^*)/(1 - x^*)] + 1) \\ \quad \times (U^* - U_f)/2 + U_f & x^* \leqslant x \leqslant 1 \end{cases} \tag{18}$$

For either function, the respective functions g_i both belong to the same four-parameter family: in eq 17, functions g_i both belong to the family of cubic polynomials; in eq 18, functions g_i both belong to the family $(\cos[\theta/a_1 + a_2])a_3 + a_4$, where $\theta = \pi(x - x^*)$ and $a_2 = 0$. Both f_1 and f_2 interpolate to function U as required by conditions 11-16 and both, having continuous first derivatives, are smooth. There is necessarily an infinite number of similarly acceptable functions because an additional, unique admissible function f_* can be formed for each unique convex linear combination of a given set of p acceptable functions (where $p \geqslant 2$) that are linearly independent, or, symbolically

$$f_*(x,x^*) = \lambda_1 f_1(x,x^*) + \lambda_2 f_2(x,x^*) + \ldots + \lambda_p f_p(x,x^*) \tag{19}$$

where $\lambda_1 + \lambda_2 + \ldots + \lambda_p = 1$ and the λ's are real numbers. For example, $f_* = \frac{1}{3} f_1 + \frac{2}{3} f_2$ is a new function satisfying all the conditions on f. Equations 17 and 18 are necessarily in terms of undetermined x^*; any interpolating function derived from eq 11-16 represents an x^*-parametrized *family* of acceptable interpolating functions f. If the single member of a family that *best* interpolates function U is to be determined, an additional condition must be imposed on the problem.

The main idea of this method is that the most realistic member of a family of interpolating functions f is the member of minimum arc length. That is, the most realistic member is the member of the family that has the least arc length for its potential curve or graph.[21] This is essentially a proposition regarding the global geometric form of the U potential curve. In this respect, it is a statement of the same type as the Hammond postulate. However, arc length is a more abstract property of the curve's form than is the property of the form addressed by the Hammond postulate, and the "nearness" or "closeness" property addressed in the postulate is subsumed in the minimum arc-length proposition: if the curve is minimized for arc length, then an activated complex and a metastable state that are near in energy are necessarily near along the x axis, hence near in structure. With reference to Figure 1, the Hammond postulate would state qualitatively that potential curve B is probably more realistic than curve A because B's associated transition state is "nearer" the final state; the arc-length minimization proposition also states that B is the more realistic, but because it is of less arc length. Clearly, the arc-length minimization proposition, in contrast to the Hammond postulate, is not limited in its application to reactions having small relative barriers in one direction (necessary for "nearness"), but applies to reactions of all exothermicities. Thus, the predictions of the Hammond postulate become a class of special cases of the more general barrier position relation derived below.

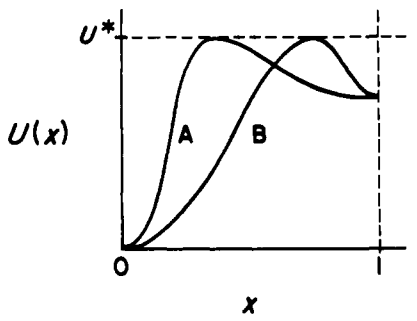

Figure 1.

The barrier position relation is the general solution of the minimization problem inherent in this interpolation procedure. Based on the above proposition, the most realistic barrier position, the maximum point of the shortest member of a family of functions f, is given directly as the zero of the function

$$\Upsilon(x^*,f) = \frac{d}{dx^*}\int_0^1 \left[1 + \left(\frac{\partial f(x,x^*)}{\partial x}\right)^2\right]^{1/2} dx \quad (20)$$

where the definite integral gives the arc length of function f on the interval $0 \leq x \leq 1$. Or equivalently, the best barrier position, symbolized x^*_0, is the solution of

$$\Upsilon(x^*,f) = 0 \quad (21)$$

Solution x^*_0 of eq 21 is itself a function of the independent variables U^* and U_f in eq 11-16, or, symbolizing the function as ψ,

$$x^*_0 = \psi(U^*,U_f) \quad (22)$$

Because of the general difficulty in finding the antiderivative in function Υ, only for very special cases of functions f of the class of eq 10 can eq 21 be solved directly in closed form to give solution ψ. However, it is a remarkable fact that *all* functions of this class have exactly the same solution ψ. This may be emphasized by rewriting eq 21 as a function independent of f, viz.,

$$\Upsilon(x^*) = 0 \quad (23)$$

which has one general solution ψ such that $\Upsilon(x^*_0) = \Upsilon(\psi(U^*,U_f)) = 0$. This result is stated as the following theorem, which has been rigorously proved by modern methods.[22]

Theorem: For all continuous functions f of the class defined in eq 10, where functions g_i belong to the same k-parameter family, the solution ψ of eq 23 is

$$x^*_0 = \frac{1}{2 - (U_f/U^*)} \quad (24)$$

if the function's $2k$ functional parameters (see definition of k-parameter family above) are uniquely determined (up to x^*) by the set of eq (a) 11-16, or (b) 11, 13-15, or (c) 11-13, 15, 16, or (d) 11, 13, 15.

Many functions, of widely varying geometric form, satisfy this theorem. Condition a of the theorem is satisfied by both functions f_1 and f_2 (eq 17 and 18), and thus the arc-length minimized barrier position is identical for both, and is given by eq 24 of the theorem. For this case $k = 4$. Condition b of the theorem applies to functions like the BEBO function that do not have stationary endpoints; an example of this type would be a potential curve formed from two concave downward parabolic segments smoothly joined with a horizontal slope at $x = x^*$. Thus, g_i would both be second degree polynomials and $k = 3$. Condition c applies to functions not having a zero first derivative at the maximum point (and therefore not being smooth), but having stationary endpoints; the intersecting concave upward parabolas employed by Marcus (see below)

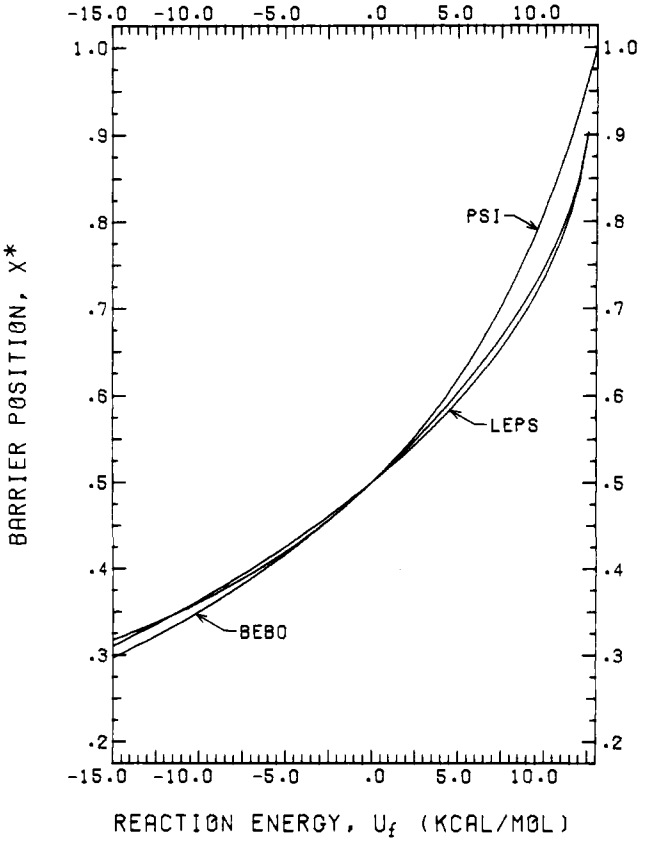

Figure 2. Functional dependency of x^* on U_f (with $U^* = 13$ kcal/mol) for relation ψ and the BEBO and LEPS potential functions.

are examples of potential curves of this type. Condition d requires that g_i both be linear functions, so that f is a sawtooth function. A variant of this simplest, special case of the theorem was proved by Heron of Alexandria by classical methods,[23] and is a cornerstone of modern optics known as Fermat's principle. The theorem as stated above is itself a restricted case of a more general statement[22] (for instance, functions g_i may themselves be defined piecewise on unequal subintervals).

Since a wide variety of admissible functions is available, *some* family of functions f can likely be found that satisfies the theorem and *one* member of which approximates a given $U(x)$ reasonably well at all values of x. But whether that well-assured, well-approximating member is indeed the shortest member as per the proposition—and therefore has its maximum point at $x = x^*_0$—must be examined for physical realism by comparison with other methods for computing the barrier position.

Comparison with Other Methods

Function ψ is tested in two general ways involving (1) the global behavior of the function itself, and (2) the saddle-point coordinates $\mathbf{R}_0(x^*)$ evaluated by the function.

Comparison of Functions. The global behavior of function ψ, eq 24, is compared below with analogous functions via comparison of the corresponding graphs. With one exception, the ψ-analogue functions are not known as explicit expressions for x^*, and the graphs were generated numerically. In Figure 2, the graph of ψ, labeled PSI, is compared with graphs of the functional dependency of the barrier position for the BEBO and LEPS potential functions, labeled BEBO and LEPS, respectively. In Figure 3, a similar comparison is made with the graphs of two ψ-analogue extensions of Marcus' relations, which are derived below. For the graphs in both figures, U^* is held constant and U_f is varied over the chemically most significant range $-U^* \leq U_f \leq U^*$.

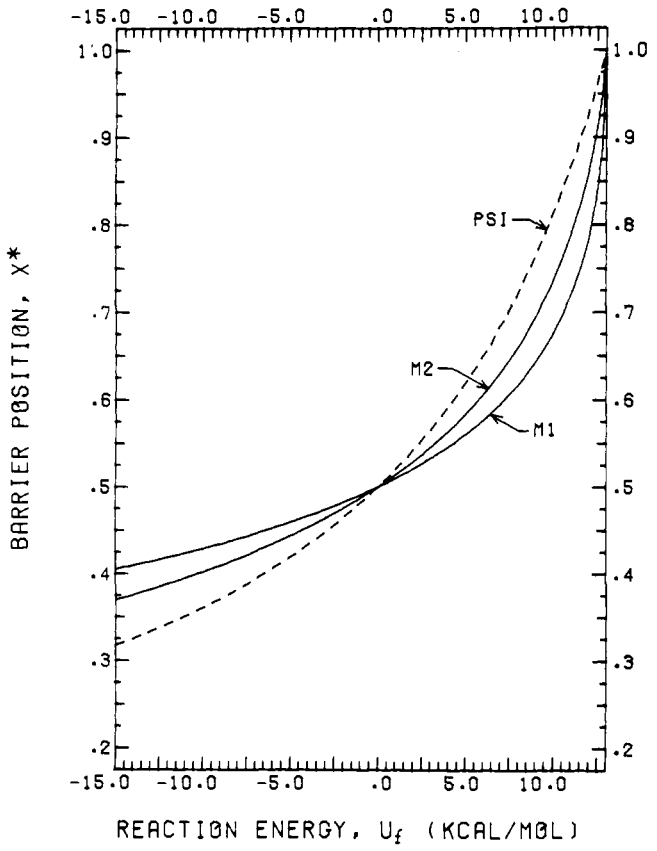

Figure 3. Functional dependency of x^* on U_f (with $U^* = 13$ kcal/mol) for relation ψ and two extensions of Marcus' relations.

(a) BEBO. The BEBO function, a semiempirical approximation to $U(x)$, was originally derived for computation of barrier heights of gas-phase H-atom transfer reactions.[15,24] According to this model, the potential energy of the three-body system in eq 3 consists of two roughly equal contributions: the energy $V_1(x)$ and $V_2(x)$ of the two bonds of the complex, and the triplet repulsion energy $V_3(x)$ between end atoms A and C. The net potential energy $V(x)$ of the system is therefore

$$V(x) = D_1 - V_1(x) - V_2(x) + V_3(x) \tag{25}$$

The terms in eq 25 are defined as follows:

$$V_1(x) = D_1(1 - x)^{p_1} \tag{26}$$

$$V_2(x) = D_2 x^{p_2} \tag{27}$$

$$V_3(x) = D_3 FB(x - x^2)^{\alpha\beta_3}[2 + B(x - x^2)^{\alpha\beta_3}] \tag{28}$$

where D_i are the (isolated) bond dissociation energies; F is the arbitrary coefficient in the Sato antibonding function taken as $F = 0.25$; α is the parameter in Pauling's relation taken as $\alpha = 0.26$; β_3 is the Morse parameter for the hypothetical AC bond;

$$p_i = \frac{\alpha \ln (D_i/\epsilon_i)}{\rho_i - \hat{r}_i} \tag{29}$$

where ϵ_i and ρ_i are bond energies and lengths, respectively, for noble-gas diatomic clusters and may be considered adjustable parameters;[15] and

$$B = \exp[-\beta_3(\hat{r}_1 + \hat{r}_2 - \hat{r}_3)] \tag{30}$$

The graph labeled BEBO in Figure 2 was generated pointwise by solving eq 25 numerically for its maximum point at 56 equally spaced values of U_f, and was plotted by the computer. U_f was varied by varying D_2, and p_2 was accordingly updated continuously via eq 29. A constant barrier height of $U^* = 13$ kcal/mol was maintained by continuously readjusting, by an iterative procedure, the triplet repulsion energy via variation of the Morse β_3 parameter. U_f could not be increased beyond about 12.6 kcal/mol, at which point all of the 13 kcal/mol barrier arose from the bonding terms V_1 and V_2. The input parameters for eq 25 were chosen so as to simulate an H-atom transfer between two carbon groups.[25]

The agreement between ψ and the analogous function for the BEBO model is very good. Actually the agreement for *bond lengths* is even better than Figure 2 suggests. Letting x^* be the position computed from the BEBO function, x^*_0 be the position computed by ψ, and Δr be the difference in the corresponding computed bond lengths of bond BC, then (from eq 6)

$$\Delta r = \alpha \ln (x^*/x^*_0) \tag{31}$$

It is clear from the figure that graphs PSI and BEBO vary together such that the ratio x^*/x^*_0 is never far from unity; thus Δr is always near zero. For example, the maximum deviation of the graphs, a difference in ordinates of about 0.08 for highly endothermic reactions of 11-12 kcal/mol, corresponds to a difference in computed activated-complex bond lengths of only 0.02 Å. Note that Δr is independent of $\hat{r}$. Although the simulation could not be extended to the endothermic limit of $U_f = U^*$, it is apparent that the BEBO ψ analogue, like ψ, is approaching the limit $x^* = 1$ as $U_f \rightarrow U^*$. This limit behavior is corroboratively consistent with the Hammond postulate.

(b) LEPS. The semiempirical LEPS function[26] is closely related to the London equation,[27] and, unlike the BEBO function, the standard expression, eq 32, evaluates the entire potential-energy surface in 4-space. Functions Q_i and J_i, the Coulomb and exchange definite integrals, respectively, are approximated via the Heitler-London method in terms of the semiempirical Morse bonding function ^1E and Sato antibonding function ^3E, so that

$$W(r_1,r_2,r_3) = \frac{1}{1+K}\Big\{Q_1(r_1) + Q_2(r_2) + Q_3(r_3) - \Big(\frac{1}{2}[J_2(r_2) - J_1(r_1)]^2 + \frac{1}{2}[J_3(r_3) - J_2(r_2)]^2 + \frac{1}{2}[J_3(r_3) - J_1(r_1)]^2\Big)^{1/2}\Big\} \tag{32}$$

$$Q_i = \frac{1}{2}[^1E_i + {}^3E_i + K(^1E_i - {}^3E_i)] \tag{33}$$

$$J_i = \frac{1}{2}[^1E_i - {}^3E_i + K(^1E_i + {}^3E_i)] \tag{34}$$

where K is Sato's empirical, adjustable parameter

$$^1E_i(r_i) = D_i\{(1 - \exp[\beta_i(\hat{r}_i - r_i)])^2 - 1\} \tag{35}$$

$$^3E_i(r_i) = FD_i\{(1 + \exp[\beta_i(\hat{r}_i - r_i)])^2 - 1\} \tag{36}$$

and $F = 0.5$.

For comparison with relation ψ and its BEBO analogue, an expression for the energy along the minimum-energy reaction path across surface W is derived assuming the validity of eq 5-7. Solving eq 6 for x and substituting same into eq 5 and 7 gives r_1 and r_3, respectively, as functions of r_2. Equations 35 and 36 may thus be rewritten as functions of one independent variable r_2:

$$^1E_1(r_2) = D_1[(1 - \{1 - \exp[(\hat{r}_2 - r_2)/\alpha]\}^{\alpha\beta_1})^2 - 1] \tag{37}$$

$$^1E_2(r_2) = D_2[(1 - \exp[\beta_2(\hat{r}_2 - r_2)])^2 - 1] \tag{38}$$

$$^1E_3(r_2) = D_3[(1 - \exp[\beta_3(\hat{r}_3 - \hat{r}_1 - r_2)]\{1 - \exp[(\hat{r}_2 - r_2)/\alpha]\}^{\alpha\beta_3})^2 - 1] \tag{39}$$

$$^3E_1(r_2) = FD_1[(1 + \{1 - \exp[(\hat{r}_2 - r_2)/\alpha]\}^{\alpha\beta_1})^2 - 1] \tag{40}$$

$$^3E_2(r_2) = FD_2[(1 + \exp[\beta_2(\hat{r}_2 - r_2)])^2 - 1] \quad (41)$$

$$^3E_3(r_2) = FD_3[(1 + \exp[\beta_3(\hat{r}_3 - \hat{r}_1 - r_2)]\{1 - \exp[(\hat{r}_2 - r_2)/\alpha]\}^{\alpha\beta_3})^2 - 1] \quad (42)$$

Substitution of eq 37-42 into eq 33 and 34 then gives from eq 32

$$W_{\mathbf{R}}(r_2) = \frac{1}{1+K}\left\{Q_1(r_2) + Q_2(r_2) + Q_3(r_2) - \left(\frac{1}{2}[J_2(r_2) - J_1(r_2)]^2 + \frac{1}{2}[J_3(r_2) - J_2(r_2)]^2 + \frac{1}{2}[J_3(r_2) - J_1(r_2)]^2\right)^{1/2}\right\} \quad (43)$$

which is the expression for the potential energy along the minimum-energy reaction path as a function of r_2. Function $W_{\mathbf{R}}(r_2)$ will be referred to as the MERP LEPS function (for minimum-energy-reaction-path LEPS). The value $K = 0.18$, as originally suggested for function W,[28] will be used for all H-atom transfer applications of $W_{\mathbf{R}}$. The function gives virtually identical results (see Table I below) for the barrier height as the three-variable function[28] $W(r_1, r_2, r_3)$, and this is good evidence for the correctness of eq 5-7.

Function $W_{\mathbf{R}}$, eq 43, was treated analogously to the BEBO function above to find x^* as a function of reaction energy U_f. The numerically generated graph, based on the same H-atom transfer simulation,[25] is shown in Figure 2 as graph LEPS. As before, the barrier height was maintained constant by continuously adjusting the repulsion energy of the end atoms via variation of the Morse parameter β_3. The maximum point of $W_{\mathbf{R}}$ was found as the zero of its first derivative, a lengthy expression solved by the secant method. The zero, $r_2(x^*)$, was converted to x^* by the inverse of eq 6. Morse constants β_1 and β_2 were evaluated by the formula[29]

$$\beta_i = 0.12177\nu_i\sqrt{\mu_i/349.76D_i} \quad (44)$$

where ν_i are the respective vibration frequencies in cm^{-1} of bonds AB and BC, both taken as 2900 cm^{-1}, and μ_i are the reduced masses. A mass of 12 amu was used for both A and C.

The comparison of ψ with the MERP LEPS analogue, as shown in Figure 2, is quantitatively similar to the comparison with the BEBO analogue. PSI and LEPS intersect at three points, allowing that they would intersect at $x^* = 1$. As with the BEBO comparison, the maximum deviation of PSI from LEPS occurs for strongly endothermic reactions of 11-12 kcal/mol. From eq 31, the maximum deviation of 0.09 corresponds to a difference in bond lengths of less than 0.03 Å.

(c) Marcus' Relations. Marcus has derived two theoretical relations for the Brønsted slope of atom transfer reactions[12] which may be reinterpreted and extended as barrier position relations analogous to ψ.

Marcus' electron transfer theory applied to atom transfer reactions establishes a relation between barrier height U^*, reaction energy U_f, and intrinsic barrier U_0, namely,

$$U^* = U_0(1 + U_f/4U_0)^2 \quad (45)$$

where $|U_f/4U_0| < 1$. Equation 45 is derived[30] straightforwardly from a model employing intersecting parabolas for the potential curve, a model, originally intended for electron transfers, which has been criticized as lacking realism when extended to atom transfer reactions.[30] The intrinsic barrier U_0 is the potential-energy barrier devoid of any "thermodynamic" contribution to its height, and in practice would be determined by extrapolation of an appropriate Brønsted plot to $U_f = 0$. If a homologous series of reactions has a constant, common U_0, then the first derivative of eq 45 with respect to U_f gives the instantaneous Brønsted slope as a function of U_f. Since the slope is equated elsewhere in Marcus' treatment to the activated-complex BC bond order of reaction 3, the first derivative may be reinterpreted as a barrier position relation,

$$x^* = \tfrac{1}{2}(1 + U_f/4U_0) \quad (46)$$

This relation may be put in terms of U^* and U_f for comparison with ψ. Solving eq 45 for U_0 and substituting the resulting expression into eq 46 gives a new relation

$$x^* = \frac{1}{2}\left(1 + \frac{U_f}{2U^* - U_f + 2\sqrt{U^*(U^* - U_f)}}\right) \quad (47)$$

which is independent of U_0.

The graph of eq 47, labeled M1, is compared with ψ in Figure 3. The two graphs are qualitatively similar; they agree exactly at $U_f = 0$ and $U_f = U^*$, but otherwise differ appreciably in their details. Comparison of Figures 2 and 3 suggests that ψ is in substantially better agreement with the BEBO and LEPS analogues than is eq 47, especially for exothermic reactions, and is probably the more realistic.

The second of Marcus' relations for the barrier height, an analogue of eq 45,

$$U^* = U_0 + \frac{U_f}{2} + \frac{U_0}{\ln 2}\ln\cosh\left(\frac{U_f \ln 2}{2U_0}\right) \quad (48)$$

is based on a simplification of the BEBO function (eq 25) in which the exponents p_i are assumed equal to unity and the triplet repulsion term V_3 is ignored. Differentiation of eq 48 with respect to U_f likewise gives a second relation for the Brønsted slope, which as above may be reinterpreted as a relation for the barrier position

$$x^* = \frac{1}{2}\left[1 + \tanh\left(\frac{U_f \ln 2}{2U_0}\right)\right] \quad (49)$$

However, U_0 cannot be eliminated from eq 49 to give an analogue of eq 47 because eq 48 cannot be solved explicitly for U_0. Nonetheless, U_0 was evaluated numerically from eq 48 for each stepwise value of U_f; the numerical solution after substitution into eq 49 allowed its ensuing, but unknown, function of U^* and U_f to be evaluated pointwise and graphed.

The graph of the unknown function based on eq 49 is labeled M2 in Figure 3. The function appears superior to eq 47 and is in better agreement with BEBO and LEPS than ψ for endothermic reactions, but not as good for exothermic reactions. It is noteworthy that both of the extensions of Marcus' relations derived above, like ψ, agree with the Hammond postulate and predict activated complexes having unit total bond order.

Comparison of Saddle-Point Coordinates of Specific Reactions. The saddle-point coordinates $\mathbf{R}_0(x^*)$ of specific reactions computed by relation ψ are compared in this section with the coordinates computed by other theoretical methods. There is no experimental method. Table I contains the r_1 and r_2 coordinates ($r_3 = r_1 + r_2$) for five reactions, covering a broad range of exothermicities, which have been studied by a variety of methods.

The methods included in the comparison are the BEBO method; the diatomics-in-molecules (DIM) method; the equibonding method, discussed below; the MERP LEPS method as above; several different semiempirical LEPS computations, collectively labeled LEPS, which individually optimize one or more dynamical parameters; the "generalized LEPS" method, which uses three adjustable parameters; the best, numerical extension of Marcus' relations, labeled M2 as in Figure 3; several diverse methods categorized simply as "semiempirical"; and quantum mechanical ab initio methods, including the configuration-interaction (CI), self-consistent-field (SCF), and unrestricted Hartree-Fock (UHF) methods.

The ψ saddle-point coordinates in Å were computed from

Table I. Saddle-Point Coordinates $r_1(x^*)$ and $r_2(x^*)$ for Five Reactions

Reaction	Method	U_f, kcal/mol	U^*, kcal/mol	r_1-(x^*), Å	r_2-(x^*), Å	Reaction	Method	U_f, kcal/mol	U^*, kcal/mol	r_1-(x^*), Å	r_2-(x^*), Å
$H_2 + Cl$	Generalized LEPS[a]	3.0	8.0	1.16	1.33	$H_2 + CH_3$	UHF[n]	3.2	29.5	0.93	1.37
	BEBO	3.1	8.0	1.09	1.35		UHF[n]	4.5	28.7	0.93	1.38
	Generalized LEPS[a]	3.0	7.7	1.11	1.35		SCF[m]	−6.7	28.5	0.86	1.42
	ψ	3.1	5.5[b]	1.05	1.37		SCF-CI[m]	−2.1	15.9	0.95	1.48
	Equibonding	3.1	12.1	0.88	1.38	$H_2 + F$	SCF[o]	13.2	29.3	0.84	1.18
	Semiempirical[c]	3.1	6.5	1.10	1.38		Equibonding	−31.8	2.2	0.79	1.21
	M2	3.1	5.5[b]	1.01	1.39		Semiempirical[p]	−31.5	1.2	0.82	1.31
	LEPS[d]	2.9	7.5	0.99	1.40		DIM[q]	−31.7	1.1	0.81	1.32
	LEPS[e]	3.1	6.7	0.98	1.40		DIM[q]	−31.7	15.5	0.82	1.39
	LEPS[a]	3.0	7.8	0.97	1.41		M2	−31.8	1.6[r]	0.77	1.51
	MERP LEPS	3.1	7.5	0.98	1.41		CI[o]	−34.4	1.7	0.77	1.54
	SCF[f]	6.7	26.2	0.94	1.46		Generalized LEPS[s]	−31.8	1.1	0.76	1.54
$H_2 + H$	Equibonding	0.0	9.8	0.86	0.86		LEPS[t]	−30.6	1.0	0.76	1.54
	Semiempirical[g]	0.0	8.6	0.90	0.90		BEBO	−31.8	1.7	0.76	1.58
	BEBO	0.0	9.8	0.92	0.92		ψ	−31.8	1.6[r]	0.75	1.72
	MERP LEPS	0.0	5.3	0.92	0.92		MERP LEPS	−31.8	0.3	0.75	1.80
	M2	0.0	8.0[h]	0.92	0.92	$F_2 + H$	SCF[u]	−132.4	12.2	1.49	1.56
	ψ	0.0	8.0[h]	0.92	0.92		SCF[v]	−130.1	13.9	1.41	1.61
	CI[i]	0.0	10.1	0.93	0.93		M2	−102.5	2.4[w]	1.43	1.64
	LEPS[j]	0.0	8.8	0.93	0.93		CI[v]	−99.0	4.1	1.50	1.68
	Semiempirical[k]	0.0	9.7	0.96	0.96		Generalized LEPS[x]	−103.4	2.4	1.44	1.90
$H_2 + CH_3$	Equibonding	−3.6	11.3	0.85	1.26		ψ	−102.5	2.4[w]	1.42	1.91
	M2	−3.6	11.6[l]	0.90	1.30		Generalized LEPS[x]	−106.7	2.3	1.42	1.96
	ψ	−3.6	11.6[l]	0.89	1.31		Generalized LEPS[x]	−87.7	2.0	1.42	1.99
	BEBO	−3.6	12.0	0.88	1.32		CI[u]	−88.4	1.0	1.57	2.05
	MERP LEPS	−3.6	5.5	0.88	1.32		Semiempirical[y]	−103.1	2.3	1.45	2.11
	SCF[m]	−14.0	23.5	0.87	1.37						

[a] A. Persky and F. S. Klein, *J. Chem. Phys.*, **44**, 3617-3626 (1966). [b] Experimental activation energy: G. C. Fettis and J. H. Knox, *Prog. React. Kinet.*, **2**, 1-38 (1964). [c] R. N. Porter, L. B. Sims, D. L. Thompson, and L. M. Raff, *J. Chem. Phys.*, **58**, 2855-2869 (1973). [d] R. L. Wilkins, *ibid.*, **63**, 2963-2969 (1975). [e] A. A. Westenberg and N. de Haas, *ibid.*, **48**, 4405-4415 (1968). [f] S. Rothenberg and H. F. Schaefer III, *Chem. Phys. Lett.*, **10**, 565-568 (1971). [g] R. N. Porter and M. Karplus, *J. Chem. Phys.*, **40**, 1105-1115 (1964). [h] Experimental activation energy: R. E. Weston, Jr., *ibid.*, **31**, 892-898 (1959). [i] B. Liu, *ibid.*, **58**, 1925-1937 (1973). [j] A. A. Westenberg and N. de Haas, *ibid.*, **47**, 1393-1405 (1967). [k] J. K. Cashion and D. R. Herschbach, *ibid.*, **40**, 2358-2363 (1964). [l] Experimental activation energy: M. J. Kurylo and R. B. Timmons, *ibid.*, **50**, 5076-5082 (1969). [m] K. Morokuma and R. E. Davis, *J. Am. Chem. Soc.*, **94**, 1060-1067 (1972). [n] S. Ehrenson and M. D. Newton, *Chem. Phys. Lett.*, **13**, 24-29 (1972). [o] C. F. Bender, S. V. O'Neil, P. K. Pearson, and H. F. Schaefer III, *Science*, **176**, 1412-1414 (1972). [p] N. C. Blais and D. G. Truhlar, *J. Chem. Phys.*, **58**, 1090-1108 (1973). [q] J. C. Tully, *ibid.*, **58**, 1396-1410 (1973). [r] Experimental activation energy: K. H. Homann, W. C. Solomon, J. Warnatz, H. Gg. Wagner, and C. Zetzsch, *Ber. Bunsenges. Phys. Chem.*, **74**, 585-589 (1970). [s] "Unpublished surface *V*:" J. T. Muckerman, Brookhaven National Laboratory, personal communication, 1977. [t] R. L. Wilkins, *J. Chem. Phys.*, **57**, 912-917 (1972). [u] S. V. O'Neil, P. K. Pearson, H. F. Schaefer III, and C. F. Bender, *ibid.*, **58**, 1126-1131 (1973). [v] C. F. Bender, C. W. Bauschlicher, Jr., and H. F. Schaefer III, *ibid.*, **60**, 3707-3708 (1974). [w] R. G. Albright, A. F. Dodonov, G. K. Lavrovskaya, I. I. Morosov, and V. L. Tal'roze, *ibid.*, **50**, 3632-3633 (1969). [x] Reference 7a. [y] Reference 7b.

eq 50 and 51 (where $U^* \geq U_f$), which were derived by substituting x^*_0 into eq 5 and 6, respectively. (Similarly, x^*, from the BEBO method and the extension of Marcus' relation, was converted to Å by eq 5 and 6.) U^* was estimated as the experimental activation energy E_a, which differs from U^* by the difference in zero-point energies of initial and activated states; U_f was determined as

$$r_1(x^*) = \hat{r}_1 + \alpha \ln\left(2 + \frac{U_f}{U^* - U_f}\right) \quad (50)$$

$$r_2(x^*) = \hat{r}_2 + \alpha \ln\left(2 - \frac{U_f}{U^*}\right) \quad (51)$$

$$U_f = D_1 - D_2 \quad (52)$$

where D_1 and D_2 are the dissociation energies D of molecules AB and BC, respectively, from the bottom of the dissociation potential well. The molecular parameters for the above and for the BEBO, MERP LEPS, and equibonding semiempirical methods are listed in Table II. The D value of 113.1 kcal/mol for CH_4 was obtained by a complete zero-point energy correction for all nine normal vibrations of CH_4 and all six of CH_3.[31,32] This fully corrected D is clearly the one that should be used in semiempirical methods such as BEBO, for otherwise the potential function will fail to give $V(1) = U_f$. In computation of the Morse β parameter for H-CH_3, the asymmetric vibration frequency was used since that motion is most akin to molecular motion along $\mathbf{R}_0$.[33] The reduced mass for H-CH_3 was computed by assuming an H atom attached to a mass of 12 amu.

Table II. Molecular Parameters

Molecule	D, kcal/mol	$\hat{r}$, Å[a]	ν, cm^{-1} [a]
H-H	109.5[b]	0.742	4395.2
H-CH_3	113.1	1.094[c]	3019.5[c]
H-F	141.3[d]	0.917	4138.5
H-Cl	106.4[e]	1.275	2989.7
F-F	38.8[f]	1.417[g]	

[a] Unless otherwise noted, see ref 29. [b] G. Herzberg and A. Monfils, *J. Mol. Spectrosc.*, **5**, 482-498 (1960). [c] Reference 32b. [d] Reference 8. [e] See footnote *a* or *e* of Table I. [f] See footnote *v* of Table I. [g] "Handbook of Chemistry and Physics", 55th ed, CRC Press, Cleveland, Ohio, 1974-1975, p F-201.

The equibonding potential function,[34] originally derived for the calculation of activation energies of gas-phase free-radical reactions, is of special interest in relation to Polanyi's equal-bonding model of the barrier position mentioned in the Introduction. In the equibonding method, the energy of the three-body complex is

Table III. Comparison of ψ-Computed $r_2(x^*)$ Coordinates with Means and Standard Deviations (sd) of Other Methods

Reaction	$r_2(x^*)$, Å (mean ± sd)	$r_2(x^*)$, Å (range for 1 sd)	$r_2(x^*)$, Å (computed by ψ)
$H_2 + Cl$	1.39 ± 0.03	1.36-1.42	1.37
$H_2 + H$	0.92 ± 0.03	0.89-0.95	0.92
$H_2 + CH_3$	1.35 ± 0.06	1.29-1.41	1.31
$H_2 + F$	1.47 ± 0.19	1.28-1.66	1.72
$F_2 + H$	1.84 ± 0.20	1.64-2.04	1.91

$$Z(r_1) = D_1 + {}^1E_1(r_1) + {}^3E_3(r_3) - E_r \qquad (53)$$

where ${}^1E_1(r_1)$ is the Morse function, ${}^3E_3(r_3)$ is the Sato triplet function with $F = 0.45$, and E_r is the resonance energy of the complex taken as a constant, 10.6 kcal/mol. In order to evaluate r_3 (the sum of r_1 and r_2), and hence evaluate ${}^3E_3(r_3)$ in eq 53, r_2 is found from the assumption of equal bonding energies by solving

$${}^1E_2(r_2) = {}^1E_1(r_1) \qquad (54)$$

for r_2. Therefore Z is a function of only one variable, r_1. The *minimum* point of $Z(r_1)$ gives the r_1 saddle-point coordinate. The present work employs a program written by the author which makes the following improvements over that previously available:[35] (a) r_2 is found as the explicit solution of eq 54 (rather than by Newton's method), and (b) the minimum point of function Z is found numerically as the zero of its first derivative (rather than by stepwise inspection). These modifications increase the computed r_2 saddle-point coordinates by 0.01 Å, or more, relative to the literature values.[34]

Table III summarizes the comparisons of Table I. The mean and standard deviation of $r_2(x^*)$ for each reaction is compared with the value computed by relation ψ. Such an analysis assumes that an entry picked at random from Table I will as likely overestimate as underestimate the true saddle-point coordinate. In Table III, for every reaction but one, the value computed by ψ lies well within one standard deviation of the mean of all the methods, and in the exceptional case, $H_2 + F$, it lies nearly within one standard deviation (1.72 vs. 1.66 Å).

Although the quantum-mechanical calculations are the most involved, the results in Tables I and III suggest they should not in general be considered definitive. The SCF method is particularly inaccurate. The inaccuracy of the latter could be surmised from its miscalculation of the barrier heights: if the *maximum* of function U is missed so badly, it is not surprising that the *maximum point* is also missed.

The equibonding method does well in computing barrier heights; however, Tables I and III suggest that it, along with the SCF method, is among the least accurate of the methods for computing the barrier position. Part of the problem is that the method does not maintain unit bond order around the transferred H atom. For example, assuming the validity of Pauling's relation, the total bond order in the H_3 activated complex is given as 1.29. Normalizing the bond order to unity brings $r_2(x^*)$ closer to the mean of the other methods, but the results are still not especially good. A simulation analogous to that of Figure 2 shows that the method is not consistent with the Hammond postulate since, although the qualitative trend is correct,[34] $x^* \not\to 1$ in the limit of $U_f = U^*$: the equibonding ψ-analogue graph, nearly a straight line, has a value $x^* = 0.806$ when $U_f = 13$ kcal/mol. The above results suggest that the equal bonding criterion by itself is inadequate to define the geometry of the true three-body activated complex (although use of different potential functions in eq 53 may give better results).

For the H-atom transfer reactions, the BEBO method is probably the best a priori method both for computing the barrier height and the barrier position. In most cases, the BEBO and MERP LEPS methods together bracket the probable true barrier *height* between them. It is therefore interesting that they generally also bracket the ψ barrier *position* between them. As Table I indicates, ψ and BEBO are very similar in their predictions of barrier position, as might be expected on the basis of Figure 2.

Conclusion

The most remarkable thing about relation ψ, eq 24, is that such a starkly simple relation could do so well. The relation agrees with the predictions of the qualitative Hammond postulate, and the minimum arc-length proposition on which ψ is based subsumes the postulate as a special case. As is shown in Figure 2, the ψ barrier position as a function of U_f behaves globally in a manner very similar to the behavior of the BEBO and LEPS potential functions. In the simulation shown in the figure, in which U_f is varied over the chemically most significant range $-U^* \leq U_f \leq U^*$, the maximum difference in the ψ and BEBO graphs corresponds to a difference in activated-complex bond lengths of only 0.02 Å; for the LEPS function the difference is similarly less than 0.03 Å. For five reactions of widely varying exothermicities whose saddle-point coordinates have been computed by a variety of methods, the coordinates computed by ψ are in good agreement with the means of all the methods, as is shown in Table III. For four of the reactions, the ψ coordinates are well within one standard deviation of the mean; for the fifth, the predicted coordinate of 1.72 Å is only slightly outside the 1.66 Å first standard deviation. As a generalization, ψ and the BEBO method—which is probably the best of the a priori methods both for computing the barrier height and the barrier position—are very similar in their predictions of barrier position. The above limited examination suggests that function ψ reliably approximates the barrier position of three-body atom transfer reactions, especially those having exothermicities in the range $-U^* \leq U_f \leq U^*$. Further testing is required, especially in regard to the relation's applicability to reactions outside the three-body class.

One utility of function ψ is its use in estimating relative activated-complex geometries for mechanistic arguments. The literature of mechanistic organic chemistry is replete with such arguments based on the less general Hammond postulate. For this purpose it is not necessary to know the complete vector equation $\mathbf{R}(x)$. That is, for mechanistically similar reactions, the relative geometries can be inferred from the relative x^* values themselves, estimated directly from ψ. For example, does a reaction with $U^* = 15$ kcal/mol and $U_f = -5$ kcal/mol have an earlier or later barrier than a mechanistically similar reaction (say both S_N2 reactions) having $U^* = 12$ kcal/mol and $U_f = -1$ kcal/mol? Relation ψ predicts that the first one, the less reactive one, will have the earlier barrier ($x^*_0 = 0.43$ vs. $x^*_0 = 0.48$). As is apparent in the expression for ψ, what is really important in determining the barrier position is not the reactivity or the exothermicity per se, but their ratio U_f/U^*.[36]

Acknowledgment. The work was initiated while holding a Molecular Dynamics Fellowship, 1974-1975, awarded by the Department of Chemistry, State University of New York at Stony Brook, and funded by the National Science Foundation. I thank Professor Bill le Noble of Stony Brook for the hospitable, stimulating environment during my year there, and for contributing to my interest in the barrier position. Most of the computational work was done at the Laboratory Computer Facility, University of Wisconsin, Madison, which was funded by the National Institutes of Health. I thank Mr. Mike Clark of LCF for providing additional computer time.

References and Notes

(1) Address correspondence to Laboratory of Molecular Biology, University of Wisconsin, Madison, Wis. 53706.
(2) For a discussion, see P. J. Kuntz in "Dynamics of Molecular Collisions," Part B, W. H. Miller, Ed., Plenum Press, New York, N.Y., 1976, Chapter 2; in particular, see pp 103 ff.
(3) (a) J. C. Polanyi and W. H. Wong, *J. Chem. Phys.*, **51**, 1439–1450 (1969); (b) N. H. Hijazi and K. J. Laidler, *ibid.*, **58**, 349–353 (1973).
(4) D. C. Wigfield and B. Lem, *Tetrahedron*, **31**, 9–11 (1975).
(5) (a) J. E. Leffler, *Science*, **117**, 340–341 (1953); (b) J. E. Leffler and E. Grunwald, "Rates and Equilibria of Organic Reactions," Wiley, New York, N.Y., 1963, pp 156–161.
(6) (a) L. B. Sims, A. Fry, L. T. Netherton, J. C. Wilson, K. D. Reppond, and S. W. Crook, *J. Am. Chem. Soc.*, **94**, 1364–1365 (1972); (b) J. Bron, *Can. J. Chem.*, **52**, 903–909 (1974).
(7) (a) N. Jonathan, S. Okuda, and D. Timlin, *Mol. Phys.*, **24**, 1143–1164 (1972); (b) R. L. Wilkins, *J. Chem. Phys.*, **58**, 2326–2332 (1973).
(8) J. T. Muckerman, *J. Chem. Phys.*, **56**, 2997–3006 (1972).
(9) G. S. Hammond, *J. Am. Chem. Soc.*, **77**, 334–338 (1955).
(10) (a) For a discussion, see J. F. Bunnett in "Investigation of Rates and Mechanisms of Reactions," Part I, 3rd ed., E. S. Lewis, Ed., Wiley, New York, N.Y., 1974, pp 466–468; (b) for a review of the use and *misuse* of the Hammond postulate, see D. Fărcasiu, *J. Chem. Educ.*, **52**, 76–79 (1975).
(11) J. C. Polanyi, *J. Chem. Phys.*, **31**, 1338–1351 (1959).
(12) R. A. Marcus, *J. Phys. Chem.*, **72**, 891–899 (1968).
(13) M. H. Mok and J. C. Polanyi, *J. Chem. Phys.*, **51**, 1451–1469 (1969).
(14) To derive eq 1, consider constructing any array of m particles. For $m = 3$, obviously $n = 3$. After three particles, for each one successively added to an array, three additional interparticle distances will completely specify the particle's relative position and therefore the configuration of the enlarged array. Hence, $n = 3 + 3j$, where j is the number of particles added after the first three. Since $j = m - 3$, $n = 3 + 3(m - 3) = 3m - 6$.
(15) H. S. Johnston and C. Parr, *J. Am. Chem. Soc.*, **85**, 2544–2551 (1963).
(16) D. G. Truhlar, *J. Am. Chem. Soc.*, **94**, 7584–7586 (1972).
(17) An MO calculation for the F-atom transfer HF + H predicts an activated-complex HF bond length of 1.14 Å; see C. F. Bender, B. J. Garrison, and H. F. Schaefer III, *J. Chem. Phys.*, **62**, 1188–1190 (1975). Pauling's relation (see text) with the assumption that bond order is conserved, and therefore $b = 0.5$, predicts in good agreement a value of 1.10 Å. Free-radical abstractions and S_N2 displacements are condensed-phase reactions possibly exhibiting conservation of bond order.
(18) See almost any reference cited in Table I.
(19) L. Pauling, *J. Am. Chem. Soc.*, **69**, 542–553 (1947). The relation is essentially eq 6 with x changed to b.
(20) The first derivative of the Morse function as a function of x is ${}^1E'_2(x) = 2D\alpha\beta_2(x^{2\alpha\beta_2-1} - x^{\alpha\beta_2-1})$; hence, ${}^1E'_2(0) = {}^1E'_2(1) = 0$. A similar expression can be written for the AB bond. For the meaning of the symbols, see text below.
(21) Naturally the absolutely shortest potential curve would consist of straight line segments; however, it is assumed, as expressed in eq 11–16, that there are additional constraints on the chemical system which preclude this. It should be noted that arc-length minimization of a coordinate function does not in general similarly minimize the vector function (**R**) of which it is a component.
(22) A. R. Miller, "An Arc Length Minimization Theorem for General Double-Knot Spline Functions", manuscript to be submitted to *Appl. Math. Optim.*
(23) See C. B. Boyer, "A History of Mathematics", Wiley, New York, N.Y., 1968, p 192.
(24) H. S. Johnston, "Gas Phase Reaction Rate Theory", Ronald Press, New York, N.Y., 1966, pp 82, 179–183, 209–214, 339–345.
(25) The reaction parameters used for both the BEBO and LEPS simulations were as follows: $D_1 = 90$ kcal/mol, $D_3 = 85$ kcal/mol, $\mathring{r}_1 = \mathring{r}_2 = 1.09$ Å, $\mathring{r}_3 = 1.54$ Å. For the BEBO simulation, the noble-gas parameters were those given by Johnston and Parr[15] and Johnston.[24]
(26) S. Sato, *J. Chem. Phys.*, **23**, 592–593 (1955).
(27) For further discussion of the method, see (a) ref 24, pp 58–62, 171–173, and 177–179, and (b) ref 7a.
(28) S. Sato, *J. Chem. Phys.*, **23**, 2465–2466 (1955).
(29) See, for example, G. Herzberg, "Molecular Spectra and Molecular Structure. I. Spectra of Diatomic Molecules", 2nd ed, Van Nostrand, New York, N.Y., 1950, p 101.
(30) G. W. Koeppl and A. J. Kresge, *Chem. Commun.*, 371–373 (1973).
(31) I thank Professor R. Claude Woods, University of Wisconsin, Madison, for suggesting the complete correction.
(32) (a) For the normal vibrations of CH_4 and CH_3, see G. Herzberg, ref 29, Vol. II, "Infrared and Raman Spectra of Polyatomic Molecules", 1945, pp 100 and 179. (b) For the corresponding frequencies for CH_4, see G. Herzberg, ref 29, Vol. III, "Electronic Spectra and Electronic Structure of Polyatomic Molecules", 1967, p 619. (c) For the corresponding frequencies for CH_3, see A. Snelson, *J. Phys. Chem.*, **74**, 537–544 (1970). (d) The zero-point energy z is given by $z = 1.4299 \times 10^{-3}\ \nu$ kcal/mol, where ν is in cm^{-1}. (e) Application of the formula in d to each vibration (some degenerate) gives a zero-point energy of 27.2 kcal/mol for CH_4 and 18.3 kcal/mol for CH_3, or a net correction of 8.9 kcal/mol. (f) The zeroth-level dissociation energy for CH_4 is 104.2 kcal/mol: J. C. Amphlett and E. Whittle, *Trans. Faraday Soc.*, **64**, 2130–2142 (1968).
(33) I thank Professor L. M. Raff, Oklahoma State University, Stillwater, for suggesting the appropriateness of this vibration.
(34) A. A. Zavitsas and A. A. Melikian, *J. Am. Chem. Soc.*, **97**, 2757–2763 (1975).
(35) I thank Professor A. A. Zavitsas, Long Island University, Brooklyn, for sending me a listing of his Program ZAV/3.
(36) NOTE ADDED IN PROOF. While this paper was in press, it was brought to my attention that a similar paper was in press elsewhere; see N. Agmon, *J. Chem. Soc., Faraday Trans. 2*, in press. In the latter, a rearranged form of eq 24 is derived and its physical realism corroborated; use of the relation is based on a symmetry principle (related to arc length minimization).

Reactive Complex Theory of Photochemical Reactions. A Nonequilibrium Approach to Chemical Rate Processes in Condensed Media

Dennis J. Diestler* and Francis K. Fong

Contribution from the Department of Chemistry, Purdue University, West Lafayette, Indiana 47907.

Received March 1, 1977

Abstract: A description of photochemical reactions in dense media is formulated in terms of the quantum statistical mechanical theory of molecular relaxation. The present formulation represents a fundamental departure from equilibrium rate theories derived from Eyring's transition-state theory. A central feature of the model is the photoactivation of a "reactive complex", which may undergo either deactivation to the ground state or reaction to yield the primary photochemical products. The theoretical description is specialized to photofragmentation reactions in solvent media. The rate constants for both deactivation and primary reaction are calculated by invoking the Born–Oppenheimer adiabatic approximation. Deactivation results from a coupling of the reaction coordinate to the center-of-mass motion of the reactive complex. Reaction, on the other hand, arises from coupling of the states of the reactive complex with those of solvent-separated fragments along the reaction coordinate itself. The theory is in qualitative accord with the results of recent picosecond time-resolved laser studies of the geminate recombination of iodine atoms in organic liquid solvents.

I. Introduction

In recent years there have been a number of developments in the quantum statistical mechanical (QSM) theory of rate processes in condensed media.[1-9] These efforts depart from conventional equilibrium rate theories derived from Eyring's transition-state theory (TST).[10-12] The principal goal of the new approach is to derive explicit expressions for the rate

0002-7863/78/1500-1992$01.00/0